THE JOURNAL OF PHYSICAL CHEMISTRY C

Article

Cite This: J. Phys. Chem. C 2019, 123, 30335−30340

pubs.acs.org/JPCC

Enhancing Oxygen Electroreduction Activity of Single-Site Fe−N−C Catalysts by a Metal Support

Zhen Jiang[†] and Vitaly Alexandrov*[,†,‡]

[†]Department of Chemical and Biomolecular Engineering and [‡]Nebraska Center for Materials and Nanoscience, University of Nebraska-Lincoln, Lincoln, Nebraska 68588, United States

Supporting Information

ABSTRACT: Development of cost-effective and highly-active platinum group metal-free (PGM-free) electrocatalysts for the oxygen reduction reaction (ORR) has recently attracted a great deal of attention. Among various PGM-free chemistries, FeN_x moieties atomically dispersed into the host carbon have emerged as promising candidates. In this work, we employ density functional theory calculations to explore the idea of ORR activity enhancement of the FeN_4 sites in the graphene matrix because of the charge transfer in a model doped graphene/metal heterostructure. By screening a number of face-centered cubic metal substrates using the computational hydrogen electrode approach, we predict Cu as a promising support that results in the theoretical ORR overpotential of the hybrid system that is lower than that of the pure Pt(111) surface. We also determine that Cu exhibits strong adhesion to the FeN_4-doped graphene that should improve stability of the catalytic system in aqueous media. Overall, the obtained results demonstrate that nanostructuring or alloying of M−N−C materials with other metals is a viable strategy to enhance the activity and stability of ORR PGM-free catalysts.

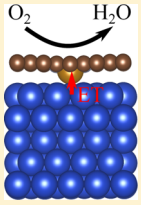

INTRODUCTION

There has been an upsurge of interest in recent years to develop platinum group metal-free (PGM-free) electrocatalysts for the oxygen reduction reaction (ORR) to replace costly precious metals used in the current polymer electrolyte fuel cell technology.[1−6] Heteroatom-doped carbon-based electrocatalysts are especially attractive as cheap and earth-abundant materials capable of delivering ORR activities approaching PGM counterparts. Such noble metal-free carbon-based catalysts are very promising because their structure is amenable to various modifications enabling efficient tuning of catalytic activity.[7−10] Despite significant progress in the field over the past years, the nature of active sites, the overall reaction mechanism, and parasitic side reactions are not well-understood. In addition, degradation of such carbon-based electrocatalysts during fuel cell operation still represents an important issue. As a result, despite the price, platinum-based catalysts remain dominant in polymer electrolyte fuel cells.

Among low-cost PGM-free electrocatalysts, two-dimensional N-doped graphene systems have been extensively explored, and a variety of doping types were studied by means of density functional theory (DFT) calculations.[11−14] Theoretical calculations suggest that single metal atoms embedded into graphene may also deliver high ORR activities.[15−19] Derived from the structure of iron porphyrin, nitrogen-doped iron and cobalt-based electrocatalysts have recently attracted a lot of interest because of their ORR activity.[20] Although the atomic structure of active sites in these materials remains largely debated,[21−24] a recent experimental study has directly identified the FeN_4 moieties in the graphene sheets,[25] advocating for the use of FeN_4 species in graphene as reasonable structural models in ab initio simulations.[26] In the case of hybrid metal−carbon systems, much of the work has been devoted to the studies of the ORR for carbon-supported metal clusters[27] and nanocomposites.[28−30] The interfacial electronic-structure changes due to the interactions between a metal nanocrystal and carbon substrate are known to be critical for the enhanced electrocatalytic activity during the ORR.

One important challenge in application of PGM-free materials is their durability which is typically inferior to that of PGM catalysts. Different deactivation mechanisms of PGM-free catalysts were previously identified including carbon corrosion, protonation of surface N groups,[31] metal dissolution,[32,33] and H_2O_2-induced degradation.[34] For example, it was recently revealed that FeN_xC_y moieties are electrochemically unstable in acidic electrolytes with respect to oxidation by H_2O_2 which is the main ORR byproduct.[34] Therefore, the design of new PGM-free material chemistries must take into account not only the reactivity but also long-term stability of catalysts in electrochemical environments.

In the present work, we aim to investigate the idea of how the reactivity of FeN_4 sites in the graphene matrix can be further enhanced by a metal substrate. We hypothesize that because of the interfacial electron transfer, the electrocatalytic activity of the FeN_4 active sites can be modulated by choosing the appropriate alloying element. We explore this idea by building a composite FeN_4-doped graphene/metal system with the (111) metal surface as a support. This model allows us to examine a series of face-centered cubic (fcc) metals that are characterized by small lattice mismatches with the graphene basal surface. Through DFT-based computational screening within the computational hydrogen electrode (CHE) ap-

Received: August 16, 2019
Revised: October 28, 2019
Published: November 22, 2019

DOI: 10.1021/acs.jpcc.9b07860
J. Phys. Chem. C 2019, 123, 30335−30340

Table 1. Structural and Energetic Parameters of the Composite FeN_4-Doped Graphene/Metal Systems[a]

		surface cell			ΔE_{adh} (eV/nm^2)			
M	D_{M-M} (Å)	a (Å)	b (Å)	mismatch (%)	atop	bridge	hollow	D_{Fe-M} (Å)
Ni	2.45	8.50	9.82	0.46	−4.84	−4.58	−4.77	2.46
Cu	2.51	8.69	10.03	1.71	−4.29	−4.37	−4.45	2.80
Ir	2.74	8.22	9.49	3.73	−3.04	−2.96	−3.05	2.79
Pd	2.78	8.34	9.63	2.33	−4.16	−4.58	−4.62	2.60
Pt	2.81	8.44	9.74	1.25	−5.86	−5.86	−5.84	2.47
Al	2.83	8.50	9.82	0.46	−2.48	−2.29	−2.27	2.71
Ag	2.96	8.88	10.25	3.92	−0.97	−1.55	−1.19	3.06
Au	2.96	8.89	10.27	4.10	−1.61	−1.83	−1.84	3.10

[a] D_{M-M} is the shortest interatomic distance for the optimized fcc metal (M) substrates and a and b are the surface cell dimensions of the corresponding metal slabs. The lattice mismatch between the doped graphene and a metal support is also listed. ΔE_{adh} stands for the adhesion energy between the carbon and metal layers, and D_{Fe-M} is the distance between the nearest metal atom of the support and the Fe atom of the FeN_4 species in the most favorable adsorption configuration.

proach, we predict that the Cu-supported FeN_4-doped graphene system has the ORR overpotential lower than that of Pt(111). We also note that Cu should be beneficial from the stability point of view because of very favorable adhesion between Cu and FeN_4-doped graphene. The remainder of this paper is organized as follows. First, we introduce the structural model and compute the ORR overpotential across a number of metal-supported FeN_4-doped graphene systems. Then, we analyze the relationship between the estimated overpotential and the electronic structure properties revealing an approximately linear correlation between the ORR overpotential and d-band center of the Fe atom.

COMPUTATIONAL DETAILS

DFT calculations were performed using the Vienna Ab initio Simulation Package (VASP)[35,36] within the generalized gradient approximation utilizing the revised Perdew–Burke–Ernzerhof (RPBE) exchange–correlation functional.[37] The RPBE functional was corrected for long-range dispersion interactions using the D3 approach according to the Grimme formalism.[38,39] A cutoff energy of 500 eV was chosen, and the convergence criteria for the total energy and atomic forces were set to 10^{-5} eV and 0.01 eV/Å, respectively. The rotationally invariant GGA + U approach was applied using the U–J values of 3.29, 3.40, and 3.87 eV on the Fe, Ni, and Cu 3d orbitals, respectively.[40,41] It should be noted that it is common to treat bulk metals using the plain GGA formalism, while GGA + U is generally reserved for application to compounds with localized electronic states such as metal oxides and nitrides. However, there were theoretical studies demonstrating that GGA + U could provide more accurate energetics for some metallic systems.[42] In the case of the FeN_4–graphene/Cu system identified as the most favorable ORR system in this work, our simulations reveal that the GGA and GGA + U calculated ORR overpotentials agree within just a few millielectronvolts. The optimized lattice parameter for each fcc metal (see Table 1 for structural information) is found to be in reasonable agreement with the literature data.[43] The periodic slab model (see Figure 1) comprising one FeN_4-doped graphene layer and five metal layers of the extended (111) surface with a vacuum gap of at least 20 Å was employed. During optimization, the bottom three layers of the metal support were fixed, while the top two layers of the metal and one graphene layer were allowed to relax. The metal bulk structures were optimized with a 12 × 12 × 12 Monkhorst–Pack mesh to sample the k-space, while the (111) metal slabs,

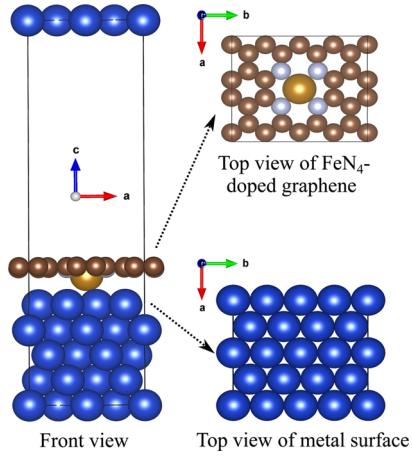

Figure 1. Simulation cell used to model the thermodynamics of the oxygen reduction reaction over the FeN_4 site of graphene supported by the (111) surface of an fcc metal using the 4 × 4 surface supercell.

FeN_4-doped graphene layer, and the composite graphene/metal systems were computed using a 4 × 3 × 1 k-point mesh.

The Gibbs free energies of the multistep ORR process were calculated according to the following equation[44–46]

$$\Delta G = \Delta E + \Delta \mathrm{ZPE} - T\Delta S$$

where ΔG is the Gibbs energy for a system under standard conditions of 298.15 K and 100 kPa. The obtained values are corrected by zero point energies (ΔZPE) and taking into consideration the entropy (ΔS) of the system at 298.15 K. Entropy values of gaseous molecules are taken from the standard tables.[47] The computational standard hydrogen electrode (SHE) approach is employed to calculate the abovementioned energy terms for the *O, *OH, and *OOH intermediates. The proton–electron pair is replaced by half of a hydrogen molecule in the SHE mode.[48] The equilibrium potential U_0 for the four-electron transfer ORR process at pH = 0 is 1.23 V versus the reversible hydrogen electrode (RHE). Therefore

$$\Delta G_{*O} = (E_{*O} + E_{H_2} - E_{H_2O} - E_*) + (\mathrm{ZPE}_{*O} + \mathrm{ZPE}_{H_2} - \mathrm{ZPE}_{H_2O} - \mathrm{ZPE}_*) - T \times (S_{*O} + S_{H_2} - S_{H_2O} - S_*)$$

DOI: 10.1021/acs.jpcc.9b07860
J. Phys. Chem. C 2019, 123, 30335–30340

$$\Delta G_{*OH} = (E_{*OH} + 0.5 \times E_{H_2} - E_{H_2O} - E_*) + (ZPE_{*OH} + 0.5 \times ZPE_{H_2} - ZPE_{H_2O} - ZPE_*) - T \times (S_{*OH} + 0.5 \times S_{H_2} - S_{H_2O} - S_*)$$

$$\Delta G_{*OOH} = (E_{*OOH} + 1.5 \times E_{H_2} - 2.0 \times E_{H_2O} - E_*) + (ZPE_{*OOH} + 1.5 \times ZPE_{H_2} - 2.0 \times ZPE_{H_2O} - ZPE_*) - T \times (S_{*OOH} + 1.5 \times S_{H_2} - 2.0 \times S_{H_2O} - S_*)$$

The Gibbs free energies for reactions 1−4 described below can be further simplified into

$$\Delta G_1 = \Delta G_{*OOH} - 4.92$$

$$\Delta G_2 = \Delta G_{*O} - \Delta G_{*OOH}$$

$$\Delta G_3 = \Delta G_{*OH} - \Delta G_{*O}$$

$$\Delta G_4 = -\Delta G_{*OH}$$

Finally, the ORR overpotential is calculated as

$$\eta = 1.23 + \max\{\Delta G_1, \Delta G_2, \Delta G_3, \Delta G_4\}/e$$

RESULTS AND DISCUSSION

Figure 1 shows the simulation cell used to model the ORR over the FeN_4 site of graphene supported by an fcc metal. Table 1 summarizes the surface cell parameters, the corresponding lattice mismatches, and the estimated adhesion energies between the metal substrate and graphene layer. It is seen that the lattice mismatch does not exceed a few percent across the chosen metals. The following equation is used to evaluate adhesion energy between the graphene layer and support

$$\Delta E_{adh} = \frac{E_{M+G} - E_M - E_G}{A}$$

where ΔE_{adh} is the adhesive energy, E_M, E_G, and E_{M+G} are the total DFT energies of a metal support, FeN_4-doped graphene, and the graphene/support heterostructure, respectively, and A is the surface area. It is seen from ΔE_{adh} reported in Table 1 that all metals exhibit propensity for binding doped graphene irrespective of the binding configuration (when Fe is positioned at the top, bridge, or hollow sites with respect to the metal surface). The highest adhesion energies are determined for Cu, Ni, and Pt suggesting enhanced stability of the corresponding composite systems with respect to degradation in electrochemical environments.

We next examine the thermodynamics of the ORR occurring at the FeN_4 catalytic site of the graphene/metal heterostructure. First of all, we estimate the Gibbs free energy of O_2 binding to the surface active site from the gas phase. Based on the calculated ΔG of O_2 adsorption at the FeN_4 site for all metal supports considered in this work, the O_2 adsorption is found to be thermodynamically unfavorable (endothermic) at room temperature. Specifically for the Cu(111) support, which turns out to exhibit the lowest theoretical ORR overpotential, ΔG (298 K, 1 bar) = 0.39 eV. The corresponding atomic structure of the adsorbed O_2 molecule at the FeN_4−graphene/Cu surface is characterized by the Fe−O distance between the Fe atom of the active site and the closest O atom in O_2 of about 2.44 Å, while the O−O distance in O_2 is 1.26 Å being very close to the value in an isolated oxygen molecule. This suggests that the chemical step of O_2 adsorption can be combined with the first electrochemical step of the ORR into a single binding/electron transfer step in agreement with some previous theoretical studies of the ORR on N-doped graphene structures.[49,50] Thus, the overall ORR mechanism can be described as a sequence of the following four H^+/e^- transfer reactions

$$* + O_{2(g)} + H^+ + e^- \rightarrow *OOH \quad (1)$$

$$*OOH + H^+ + e^- \rightarrow H_2O + *O \quad (2)$$

$$*O + H^+ + e^- \rightarrow *OH \quad (3)$$

$$*OH + H^+ + e^- \rightarrow H_2O + * \quad (4)$$

where * indicates the catalyst surface and *X represents a chemical moiety bound to the surface active site.

The calculated Gibbs free energies of the abovementioned four-electron transfer reactions (ΔG_1, ΔG_2, ΔG_3, and ΔG_4) reveal that the adsorption of OOH species (characterized by ΔG_1) is always the potential-determining step (PDS) of the overall ORR process for all the metal substrates except Ir (see Table 2). As seen from the calculated ΔG_1 listed in Table S2 (Supporting Information), the adsorption strength of the Fe center for OOH is gradually increasing when going from Pd and Au to Cu. To elucidate the reason for such behavior, we plot the electron density difference maps (EDDMs) for the Au and Cu cases (Figure 2). It can be seen that the Cu support unlike Au provides more electron density to the Fe atom forming a tighter Fe−OOH bond. The more pronounced charge transfer across the interface in the case of Cu is also illustrated by the density of states (DOS) (Figure 3), revealing a more substantial overlap between the Fe 3d and O 2p orbitals as compared to the Au case.

Table 2. Estimated Values of the d-Band Center of the Fe Atom DOS in the Doped Graphene/Metal Heterostructure, the PDS of the ORR, and the Corresponding Theoretical Overpotential (η)

M	d band center (eV)	PDS	η (V)
Cu	−1.30	1	0.44
Al	−1.64	1	0.52
Ag	−1.66	1	0.54
Ni	−1.37	1	0.64
Pt	−1.82	1	0.84
Au	−1.73	1	0.84
Ir	−1.85	2	0.97
Pd	−2.39	1	1.08

The obtained theoretical values of the ORR overpotential (η) for the studied systems are listed in Table 2. The lowest overpotential is found for the system with the Cu substrate (0.44 V), and the highest overpotential is computed for Pd (1.08 V). We note that the predicted η for the Cu system is even lower than the one computed for the pristine Pt(111) surface (~0.5 V for a 2 × 2 surface cell). The overpotential is

DOI: 10.1021/acs.jpcc.9b07860
J. Phys. Chem. C 2019, 123, 30335−30340

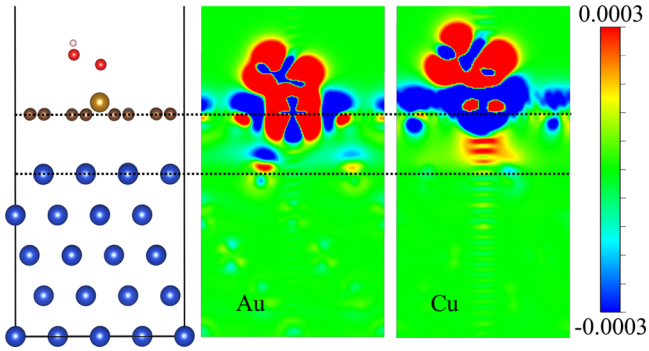

Figure 2. Two-dimensional EDDMs for the OOH adsorbed over the FeN_4 center for Cu and Au substrates. The red indicates electron density depletion, while the blue indicates electron density accumulation.

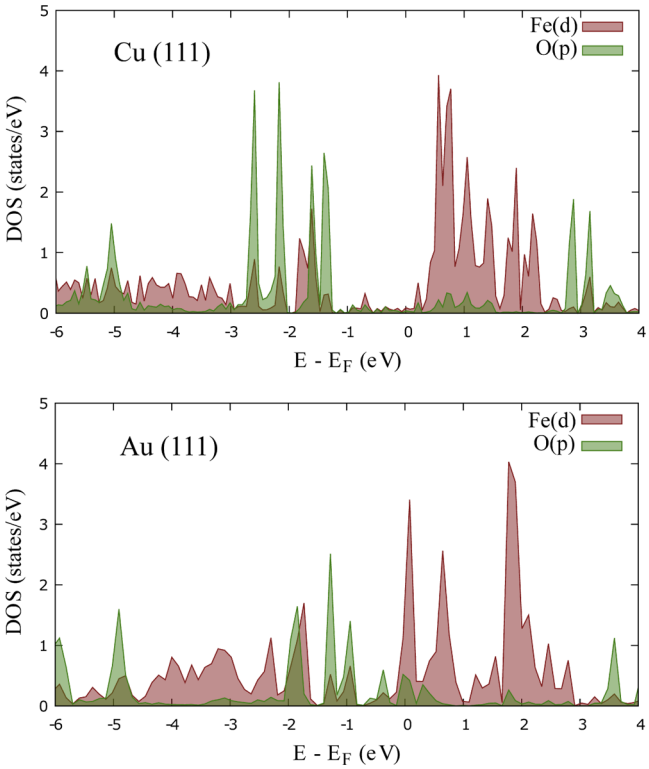

Figure 3. DOS projected onto the Fe and adjacent O atoms when OOH is adsorbed at the FeN_4 site of graphene supported by Cu (upper panel) and Au (lower panel).

also low for the Al case, but Al should be easily oxidized under ORR operating conditions. The inclusion of implicit water solvation using the VASPsol implementation[51] reveals that the stabilization energy for the adsorbed OOH intermediate due to the solvent is comparable to previous theoretical results on the ORR over doped graphene (~0.2−0.3 eV).[41,52] We also find that OOH is slightly more stabilized by the implicit solvent in the case of the doped graphene/Cu system than for the pristine Pt(111) surface (by ~0.06 eV). Because a larger surface cell may be required to avoid defect self-interaction, we also estimated the ORR overpotential using a 6 × 6 surface cell in the case of the Cu support resulting in a slightly increased value of 0.47 V. We determine, however, that the ORR overpotential would also increase for the pristine Pt(111) surface if using a larger 6 × 6 surface cell leading to the value of about 0.6 V.

Furthermore, we correlate the obtained overpotentials with the d-band centers of the Fe atom across the graphene/metal systems and find a nearly linear relationship between the two quantities as demonstrated in Figure 4. The figure shows that

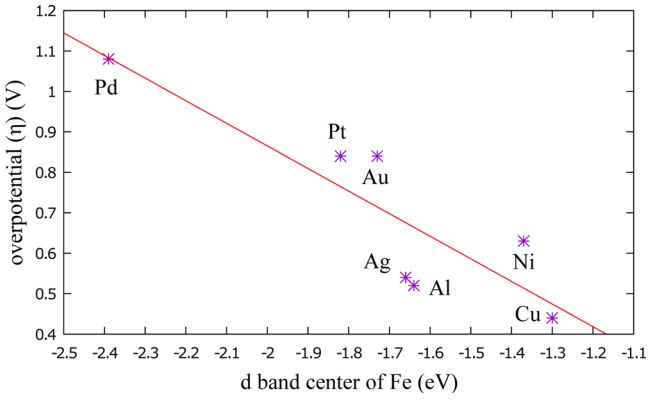

Figure 4. Linear correlation plot between the theoretical ORR overpotential and d-band center of the Fe atom across the composite systems under study.

the overpotential decreases with an increase of the d-band center of the Fe atom and therefore the d-band center approach can be used to screen ORR candidates beyond the systems examined in this work. This relationship is in agreement with the fact that the higher d-band center of a transition metal should result in a higher activity for adsorption of water species.

CONCLUSIONS

In this work, we have investigated the idea of possible enhancement of electrocatalytic activity of the PGM-free FeN_4-doped graphene by a metal support toward the ORR. To this end, we have employed the DFT-based CHE approach to predict the ORR overpotential across a number of fcc metals. The obtained results suggest Cu as a promising metal support that gives rise to the ORR overpotential of about 0.44 V which is lower than that of the pristine Pt(111) surface. A linear correlation between the estimated ORR overpotential and the d-band center of the Fe active site is found, which can be used for screening other metals to catalyze the ORR. In addition, Cu is determined to exhibit high adhesion with FeN_4-doped graphene that should improve stability of the composite system under aqueous electrochemical conditions. Overall, these results suggest that coupling Fe−N−C catalysts with metals through nanostructuring or alloying to produce composite structures should be a feasible strategy for facilitating the ORR.

ASSOCIATED CONTENT

Supporting Information

The Supporting Information is available free of charge at https://pubs.acs.org/doi/10.1021/acs.jpcc.9b07860.

Gibbs free energies of *O, *OH, and *OOH adsorbed on the FeN_4-doped graphene supported by fcc metal(111) surfaces, Gibbs free energies of reactions (1−4) on the FeN_4-doped graphene supported by fcc metal(111) surfaces, and optimized geometries of FeN_4-doped graphene supported by Cu (PDF)

DOI: 10.1021/acs.jpcc.9b07860
J. Phys. Chem. C 2019, 123, 30335−30340

AUTHOR INFORMATION

Corresponding Author

*E-mail: valexandrov2@unl.edu. Phone: +1 402 4725323.

ORCID

Zhen Jiang: 0000-0002-1175-5658

Vitaly Alexandrov: 0000-0003-2063-6914

Notes

The authors declare no competing financial interest.

ACKNOWLEDGMENTS

The Holland Computing Center at the University of Nebraska-Lincoln is acknowledged for computational support. In addition, we are grateful to Nadia Intan and Qiong Yang for useful discussion.

REFERENCES

(1) Lefèvre, M.; Proietti, E.; Jaouen, F.; Dodelet, J.-P. Iron-based catalysts with improved oxygen reduction activity in polymer Electrolyte Fuel Cells. *Science* **2009**, *324*, 71−74.

(2) Lv, H.; Li, D.; Strmcnik, D.; Paulikas, A. P.; Markovic, N. M.; Stamenkovic, V. R. Recent advances in the design of tailored nanomaterials for efficient oxygen reduction reaction. *Nano Energy* **2016**, *29*, 149−165.

(3) Martinez, U.; Komini Babu, S.; Holby, E. F.; Chung, H. T.; Yin, X.; Zelenay, P. Progress in the development of Fe-based PGM-free electrocatalysts for the oxygen reduction reaction. *Adv. Mater.* **2019**, *31*, 1806545.

(4) Dembinska, B.; Brzozowska, K.; Szwed, A.; Miecznikowski, K.; Negro, E.; Di Noto, V.; Kulesza, P. J. Electrocatalytic oxygen reduction in alkaline medium at graphene-supported silver-iron carbon nitride sites generated during thermal decomposition of silver hexacyanoferrate. *Electrocatalysis* **2019**, *10*, 112−124.

(5) Gewirth, A. A.; Varnell, J. A.; DiAscro, A. M. Nonprecious metal catalysts for oxygen reduction in heterogeneous aqueous systems. *Chem. Rev.* **2018**, *118*, 2313−2339.

(6) Omasta, T. J.; Peng, X.; Miller, H. A.; Vizza, F.; Wang, L.; Varcoe, J. R.; Dekel, D. R.; Mustain, W. E. Beyond 1.0 W cm- 2 performance without platinum: The beginning of a new era in anion exchange membrane fuel cellsBeyond 1.0 W cm−2Performance without Platinum: The Beginning of a New Era in Anion Exchange Membrane Fuel Cells. *J. Electrochem. Soc.* **2018**, *165*, J3039−J3044.

(7) Dumont, J. H.; Martinez, U.; Artyushkova, K.; Purdy, G. M.; Dattelbaum, A. M.; Zelenay, P.; Mohite, A.; Atanassov, P.; Gupta, G. Nitrogen-doped graphene oxide electrocatalysts for the oxygen reduction reaction. *ACS Appl. Nano Mater.* **2019**, *2*, 1675−1682.

(8) Feng, L.-Y.; Liu, Y.-J.; Zhao, J.-X. Iron-embedded boron nitride nanosheet as a promising electrocatalyst for the oxygen reduction reaction (ORR): a density functional theory (DFT) study. *J. Power Sources* **2015**, *287*, 431−438.

(9) Jaouen, F.; Proietti, E.; Lefèvre, M.; Chenitz, R.; Dodelet, J.-P.; Wu, G.; Chung, H. T.; Johnston, C. M.; Zelenay, P. Recent advances in non-precious metal catalysis for oxygen-reduction reaction in polymer electrolyte fuel cells. *Energy Environ. Sci.* **2011**, *4*, 114−130.

(10) Ha, Y.; Kang, S.; Ham, K.; Lee, J.; Kim, H. Experimental and density functional theory corroborated optimization of durable metal embedded carbon nanofiber for oxygen electrocatalysis. *J. Phys. Chem. Lett.* **2019**, *10*, 3109−3114.

(11) Holby, E. F.; Taylor, C. D. Control of graphene nanoribbon vacancies by Fe and N dopants: Implications for catalysis. *Appl. Phys. Lett.* **2012**, *101*, 064102.

(12) Zhang, L.; Niu, J.; Dai, L.; Xia, Z. Effect of microstructure of nitrogen-doped graphene on oxygen reduction activity in fuel cells. *Langmuir* **2012**, *28*, 7542−7550.

(13) Dombrovskis, J. K.; Palmqvist, A. E. C. Recent progress in synthesis, characterization and evaluation of non-precious metal catalysts for the oxygen reduction reaction. *Fuel Cells* **2016**, *16*, 4−22.

(14) Anderson, A. B.; Holby, E. F. Pathways for O_2 Electroreduction over Substitutional FeN_4, $HOFeN_4$, and $OFeN_4$ in Graphene Bulk Sites: Critical Evaluation of Overpotential Predictions Using LGER and CHE Models. *J. Phys. Chem. C* **2019**, *123*, 18398−18409.

(15) Wu, G.; More, K. L.; Johnston, C. M.; Zelenay, P. High-performance electrocatalysts for oxygen reduction derived from polyaniline, iron, and cobalt. *Science* **2011**, *332*, 443−447.

(16) Fan, L.; Liu, P. F.; Yan, X.; Gu, L.; Yang, Z. Z.; Yang, H. G.; Qiu, S.; Yao, X. Atomically isolated nickel species anchored on graphitized carbon for efficient hydrogen evolution electrocatalysis. *Nat. Commun.* **2016**, *7*, 10667.

(17) Fei, H.; Dong, J.; Arellano-Jiménez, M. J.; Ye, G.; Kim, N. D.; Samuel, E. L.; Peng, Z.; Zhu, Z.; Qin, F.; Bao, J.; et al. Atomic cobalt on nitrogen-doped graphene for hydrogen generation. *Nat. Commun.* **2015**, *6*, 8668.

(18) Chen, X.; Chen, S.; Wang, J. Screening of catalytic oxygen reduction reaction activity of metal-doped graphene by density functional theory. *Appl. Surf. Sci.* **2016**, *379*, 291−295.

(19) Chen, Y.; Ji, S.; Wang, Y.; Dong, J.; Chen, W.; Li, Z.; Shen, R.; Zheng, L.; Zhuang, Z.; Wang, D.; et al. Isolated single iron atoms anchored on N-doped porous carbon as an efficient electrocatalyst for the oxygen reduction reaction. *Angew. Chem., Int. Ed.* **2017**, *56*, 6937−6941.

(20) Martinez, U.; Holby, E. F.; Babu, S. K.; Artyushkova, K.; Lin, L.; Choudhury, S.; Purdy, G. M.; Zelenay, P. Experimental and Theoretical Trends of PGM-Free Electrocatalysts for the Oxygen Reduction Reaction with Different Transition Metals. *J. Electrochem. Soc.* **2019**, *166*, F3136−F3142.

(21) Zhang, L.; Xia, Z. Mechanisms of oxygen reduction reaction on nitrogen-doped graphene for fuel cells. *J. Phys. Chem. C* **2011**, *115*, 11170−11176.

(22) Artyushkova, K.; Serov, A.; Rojas-Carbonell, S.; Atanassov, P. Chemistry of Multitudinous Active Sites for Oxygen Reduction Reaction in Transition Metal-Nitrogen-??Carbon Electrocatalysts. *J. Phys. Chem. C* **2015**, *119*, 25917−25928.

(23) Buan, M. E. M.; Cognigni, A.; Walmsley, J. C.; Muthuswamy, N.; Rønning, M. Active sites for the oxygen reduction reaction in nitrogen-doped carbon nanofibers. *Catal. Today* **2019**, DOI: 10.1016/j.cattod.2019.01.018.

(24) Sohrabi, S.; Ghalkhani, M. Metal−Organic Frameworks as Electro-Catalysts for Oxygen Reduction Reaction in Electrochemical Technologies. *J. Electron. Mater.* **2019**, *48*, 4127−4137.

(25) Chung, H. T.; Cullen, D. A.; Higgins, D.; Sneed, B. T.; Holby, E. F.; More, K. L.; Zelenay, P. Direct atomic-level insight into the active sites of a high-performance PGM-free ORR catalyst. *Science* **2017**, *357*, 479−484.

(26) Holby, E. F.; Wu, G.; Zelenay, P.; Taylor, C. D. Structure of Fe−N_x−C Defects in Oxygen Reduction Reaction Catalysts from First-Principles Modeling. *J. Phys. Chem. C* **2014**, *118*, 14388−14393.

(27) Liang, Y.; Li, Y.; Wang, H.; Zhou, J.; Wang, J.; Regier, T.; Dai, H. Co 3 O 4 nanocrystals on graphene as a synergistic catalyst for oxygen reduction reaction. *Nat. Mater.* **2011**, *10*, 780.

(28) Seger, B.; Kamat, P. V. Electrocatalytically active graphene-platinum nanocomposites. Role of 2-D carbon support in PEM fuel cells. *J. Phys. Chem. C* **2009**, *113*, 7990−7995.

(29) Palaniselvam, T.; Kashyap, V.; Bhange, S. N.; Baek, J.-B.; Kurungot, S. Nanoporous graphene enriched with Fe/Co-N active sites as a promising oxygen reduction electrocatalyst for anion exchange membrane fuel cells. *Adv. Funct. Mater.* **2016**, *26*, 2150−2162.

(30) Peng, X.; Omasta, T. J.; Magliocca, E.; Wang, L.; Varcoe, J. R.; Mustain, W. E. Nitrogen-doped carbon−CoO_x nanohybrids: a precious metal free cathode that exceeds 1.0 W cm^{-2} peak power and 100 h life in anion-exchange membrane fuel cells. *Angew. Chem., Int. Ed.* **2019**, *58*, 1046−1051.

(31) Herranz, J.; Jaouen, F.; Lefèvre, M.; Kramm, U. I.; Proietti, E.; Dodelet, J.-P.; Bogdanoff, P.; Fiechter, S.; Abs-Wurmbach, I.; Bertrand, P.; et al. Unveiling N-protonation and anion-binding effects

DOI: 10.1021/acs.jpcc.9b07860
J. Phys. Chem. C 2019, 123, 30335−30340

on Fe/N/C catalysts for O_2 reduction in proton-exchange-membrane fuel cells. *J. Phys. Chem. C* **2011**, *115*, 16087−16097.
(32) Ferrandon, M.; Wang, X.; Kropf, A. J.; Myers, D. J.; Wu, G.; Johnston, C. M.; Zelenay, P. Stability of iron species in heat-treated polyaniline-iron-carbon polymer electrolyte fuel cell cathode catalysts. *Electrochim. Acta* **2013**, *110*, 282−291.
(33) Santori, P. G.; Speck, F. D.; Li, J.; Zitolo, A.; Jia, Q.; Mukerjee, S.; Cherevko, S.; Jaouen, F. Effect of pyrolysis atmosphere and electrolyte pH on the oxygen reduction activity, stability and spectroscopic signature of FeN_x moieties in Fe-N-C catalysts. *J. Electrochem. Soc.* **2019**, *166*, F3311−F3320.
(34) Choi, C. H.; Lim, H.-K.; Chung, M. W.; Chon, G.; Ranjbar Sahraie, N.; Altin, A.; Sougrati, M.-T.; Stievano, L.; Oh, H. S.; Park, E. S.; et al. The Achilles' heel of iron-based catalysts during oxygen reduction in an acidic medium. *Energy Environ. Sci.* **2018**, *11*, 3176−3182.
(35) Kresse, G.; Furthmüller, J. Efficiency of ab-initio total energy calculations for metals and semiconductors using a plane-wave basis set. *Comput. Mater. Sci.* **1996**, *6*, 15−50.
(36) Kresse, G.; Furthmüller, J. Efficient iterative schemes for ab initio total-energy calculations using a plane-wave basis set. *Phys. Rev. B: Condens. Matter Mater. Phys.* **1996**, *54*, 11169.
(37) Perdew, J. P.; Burke, K.; Ernzerhof, M. Generalized gradient approximation made simple. *Phys. Rev. Lett.* **1996**, *77*, 3865.
(38) Grimme, S.; Antony, J.; Ehrlich, S.; Krieg, H. A consistent and accurate ab initio parametrization of density functional dispersion correction (DFT-D) for the 94 elements H-Pu. *J. Chem. Phys.* **2010**, *132*, 154104.
(39) Grimme, S.; Ehrlich, S.; Goerigk, L. Effect of the damping function in dispersion corrected density functional theory. *J. Comput. Chem.* **2011**, *32*, 1456−1465.
(40) Dudarev, S. L.; Botton, G. A.; Savrasov, S. Y.; Humphreys, C. J.; Sutton, A. P. Electron-energy-loss spectra and the structural stability of nickel oxide: An LSDA+ U study. *Phys. Rev. B: Condens. Matter Mater. Phys.* **1998**, *57*, 1505.
(41) Xu, H.; Cheng, D.; Cao, D.; Zeng, X. C. A universal principle for a rational design of single-atom electrocatalysts. *Nat. Catal.* **2018**, *1*, 339.
(42) Xie, W.; Xiong, W.; Marianetti, C. A.; Morgan, D. Correlation and relativistic effects in U metal and U-Zr alloy: Validation of ab initio approaches. *Phys. Rev. B: Condens. Matter Mater. Phys.* **2013**, *88*, 235128.
(43) Janthon, P.; Luo, S.; Kozlov, S. M.; Viñes, F.; Limtrakul, J.; Truhlar, D. G.; Illas, F. Bulk properties of transition metals: a challenge for the design of universal density functionals. *J. Chem. Theory Comput.* **2014**, *10*, 3832−3839.
(44) Rossmeisl, J.; Qu, Z.-W.; Zhu, H.; Kroes, G.-J.; Nørskov, J. K. Electrolysis of water on oxide surfaces. *J. Electroanal. Chem.* **2007**, *607*, 83−89.
(45) Nørskov, J. K.; Rossmeisl, J.; Logadottir, A.; Lindqvist, L.; Kitchin, J. R.; Bligaard, T.; Jonsson, H. Origin of the overpotential for oxygen reduction at a fuel-cell cathode. *J. Phys. Chem. B* **2004**, *108*, 17886−17892.
(46) Rossmeisl, J.; Logadottir, A.; Nørskov, J. K. Electrolysis of water on (oxidized) metal surfaces. *Chem. Phys.* **2005**, *319*, 178−184.
(47) Atkins, P.; De Paula, J.; Keeler, J. *Physical Chemistry*; Oxford university press, 2018.
(48) Man, I. C.; Su, H.-Y.; Calle-Vallejo, F.; Hansen, H. A.; Martínez, J. I.; Inoglu, N. G.; Kitchin, J.; Jaramillo, T. F.; Nørskov, J. K.; Rossmeisl, J. Universality in oxygen evolution electrocatalysis on oxide surfaces. *ChemCatChem* **2011**, *3*, 1159−1165.
(49) Chai, G.-L.; Hou, Z.; Shu, D.-J.; Ikeda, T.; Terakura, K. Active sites and mechanisms for oxygen reduction reaction on nitrogen-doped carbon alloy catalysts: Stone-Wales defect and curvature effect. *J. Am. Chem. Soc.* **2014**, *136*, 13629−13640.
(50) Holby, E. F.; Zelenay, P. Linking structure to function: The search for active sites in non-platinum group metal oxygen reduction reaction catalysts. *Nano Energy* **2016**, *29*, 54−64.
(51) Mathew, K.; Sundararaman, R.; Letchworth-Weaver, K.; Arias, T. A.; Hennig, R. G. Implicit solvation model for density-functional study of nanocrystal surfaces and reaction pathways. *J. Chem. Phys.* **2014**, *140*, 084106.
(52) Calle-Vallejo, F.; Martínez, J. I.; García-Lastra, J. M.; Abad, E.; Koper, M. T. M. Oxygen reduction and evolution at single-metal active sites: Comparison between functionalized graphitic materials and protoporphyrins. *Surf. Sci.* **2013**, *607*, 47−53.

DOI: 10.1021/acs.jpcc.9b07860
J. Phys. Chem. C 2019, 123, 30335−30340